

Qatten: A General Framework for Cooperative Multiagent Reinforcement Learning

Yaodong Yang¹ Jianye Hao¹ Ben Liao² Kun Shao³ Guangyong Chen² Wulong Liu³ Hongyao Tang¹

Abstract

In many real-world settings, a team of cooperative agents must learn to coordinate their behavior with private observations and communication constraints. Deep multiagent reinforcement learning algorithms (Deep-MARL) have shown superior performance in these realistic and difficult problems but still suffer from challenges. One branch is the multiagent value decomposition, which decomposes the global shared multiagent Q-value Q_{tot} into individual Q-values Q^i to guide individuals' behaviors. However, previous work achieves the value decomposition heuristically without valid theoretical groundings, where VDN supposes an additive formation and QMIX adopts an implicit inexplicable mixing method. In this paper, for the first time, we theoretically derive a linear decomposing formation from Q_{tot} to each Q^i . Based on this theoretical finding, we introduce the multi-head attention mechanism to approximate each term in the decomposing formula with theoretical explanations. Experiments show that our method outperforms state-of-the-art MARL methods on the widely adopted StarCraft benchmarks across different scenarios, and attention analysis is also investigated with sights.

1. Introduction

Cooperative multiagent reinforcement learning problem has been studied extensively in the last decade, where a system of agents learn towards coordinated policies to optimize the accumulated global rewards (Busoniu et al., 2008; Gupta et al., 2017; Palmer et al., 2018). Complex tasks such as the coordination of autonomous vehicles (Cao et al., 2012), optimizing the productivity of a factory in distributed logistics (Ying & Sang, 2005) and energy distribution, often modeled as cooperative multi-agent learning problems, have great

application prospect and enormous commercial value.

One natural way to address cooperative MARL problem is the centralized approach, which views the multiagent system (MAS) as a whole and solves it as a single-agent learning task. In such settings, existing reinforcement learning (RL) techniques can be leveraged to learn joint optimal policies based on agents joint observations and common rewards (Tan, 1993). However, the centralized approach usually scales not well, since the joint action space of agents grows exponentially as the increase of the number of agents. Furthermore, partial observation limitation and communication constraints also necessitate the learning of decentralised policies, which condition only on the local action-observation history of each agent (Foerster et al., 2018).

Another choice is the decentralized approach that each agent learns its own policy. Letting individual agents learn concurrently based on the global reward (aka. independent learners) (Tan, 1993) is the simplest option. However, it shown to be difficult in even simple two-agent, single-state stochastic coordination problems. One main reason is that the global reward signal brings the non-stationarity that agents cannot distinguish between the stochasticity of the environment and the exploitative behaviors of other co-learners (Lowe et al., 2017), and thus may mistakenly update their policies. To mitigate this issue, decentralized policies can often be learned in the centralized training with decentralized execution (CTDE) paradigm. Whiling training, a centralized critic could be accessible to the joint action and additional state information to give update signals for decentralized agent polices, which only receive its local observations for deployment. For CTDE, one major challenge is how to represent and use the centralized multiagent action-value function Q_{tot} . Such a complex function is difficult to learn when there are many agents and, even if it can be learned, offers no obvious way to induce decentralized policies that allow each agent to act based on an individual observation.

We can learn a fully centralized state-action value function Q_{tot} and then use it to guide the optimization of decentralised policies in an actor-critic framework, an approach taken by counterfactual multi-agent (COMA) policy gradients (Foerster et al., 2018), as well as work by (Gupta et al., 2017). However, the fully centralized critic of COMA suf-

¹Tianjin Univeristy, China ²Tencent, China ³Huawei Noah's Ark Lab, China. Correspondence to: Jianye Hao <jianye.hao@tju.edu.cn>.

fers difficulty in evaluating global Q-values from the joint state-action space especially when there are more than a handful of agents and is hard to give an appropriate multi-agent baseline (Schroeder de Witt et al., 2019).

Different from previous methods, Value Decomposition Network (VDN) (Sunehag et al., 2018) is proposed to learn a centralized but factored Q_{tot} in between these two extremes. By representing Q_{tot} as a sum of individual value functions Q^i that condition only on individual observations and actions, a decentralized policy arises simply from each agent selecting actions greedily with respect to its Q^i . However, VDN supposes a strict additive assumption between Q_{tot} and Q^i , and ignores any extra state information available during training. Later QMIX is proposed to overcome the limitations of VDN (Rashid et al., 2018). QMIX employs a network that estimates joint action-values as a black-box non-linear combination of per-agent values that condition only on local observations. Besides, QMIX enforces that Q_{tot} is monotonic in Q^i , which allows computationally tractable maximisation of the joint action-value in off-policy learning. But QMIX performs an implicit mixing of Q^i and regards the mixing process as a black-box. Both VDN and QMIX introduce the representation limitations with the assumptions of the additive or monotonic relationship of Q_{tot} and Q^i . Recently, QTRAN is proposed to guarantee optimal decentralization by using linear constraints while avoiding representation limitations introduced by VDN and QMIX. However, the constraints of QTRAN on the optimization problem involved is computationally intractable and authors have to relax these constraints by two penalties thus deviate QTRAN from exact solutions (Mahajan et al., 2019).

In this paper, for the first time, we theoretically derive a generalized formalization of Q_{tot} and Q^i for any number of cooperative agents (Theorem 2 and 3) without introducing additional assumptions or constraints. Following the theoretical formalization, we also propose a practical multi-head attention based Q-value mixing network (Qatten) to approximate the global Q-value and the decomposition of individual Q-values. Qatten takes advantages of the key-value memory operation to measure the importance of each agent for the global system and the multi-head structure to capture the different high-order partial derivatives of Q_{tot} with respect to Q^i when decomposing. Besides, Qatten can be enhanced by the weighted head Q-value and non-linearity mechanisms for greater approximation ability. Experiments on the challenging MARL benchmark show that our method obtains the best performance. The attention analysis shows that Qatten captures the importance of each agent properly for approximating Q_{tot} and, to some degree, reveals the internal workflow of the Q_{tot} 's approximation from Q^i .

The remainder of this paper is organized as follows. We first introduce the Markov games, Deep-MARL algorithms and

attention mechanism in Section 2. Then in Section 3, we explain the explicit formula for local behavior of cooperative MARL and derive the mathematical relation between Q_{tot} and Q^i . Next, in Section 4, we present the framework of Qatten in details. Furthermore, we validate Qatten in the challenging StarCraft II platform and give the specific analysis including the multi-head attention in Section 5. Finally, conclusions and future work are provided in Section 6.

2. Background

2.1. Markov Games

Markov games is a multi-agent extension of Markov Decision Processes (Littman, 1994). They are defined by a set of states, S , action sets for each of N agents, A^1, \dots, A^N , a state transition function, $T : S \times A^1 \times \dots \times A^N \rightarrow P(S)$, which defines the probability distribution over possible next states, given the current state and actions for each agent, and a reward function for each agent that also depends on the global state and actions of all agents, $R^i : S \times A^1 \times \dots \times A^N \rightarrow \mathbb{R}$. We specially consider the partial observed Markov games, in which each agent i receives a local observation $o^i : Z(S, i) \rightarrow O^i$. Each agent learns a policy $\pi^i : O^i \rightarrow P(A^i)$ which maps each agent's observation to a distribution over its action set. Each agent learns a policy that maximizes its expected discounted returns, $J^i(\pi^i) = \mathbb{E}_{a^1 \sim \pi^1, \dots, a^N \sim \pi^N, s \sim T} [\sum_{t=0}^{\infty} \gamma^t r_t^i(s_t, a_t^1, \dots, a_t^N)]$, where $\gamma \in [0, 1]$ is the discounted factor. If all agents receive the same rewards ($R^1 = \dots = R^N = R$), Markov games becomes fully-cooperative: a best-interest action of one agent is also a best-interest action of others (Matignon et al., 2012). We consider the fully-cooperative partially observed Markov games in this paper. For the partially observed Markov games, an empirical centralized training, decentralized execution paradigm (Lowe et al., 2017) is employed to train well-coordinated decentralized policies by incorporating the global information when training in the simulation.

2.2. Centralized Training with Decentralized Execution

Arguably the most naive training method for MARL tasks is to learn the individual agents action-value functions independently, i.e., independent Q-learning. This method would be simple and scalable, but it shown to be difficult in even simple two-agent, single-state stochastic coordination problems (Tan, 1993). Recently, for Markov games especially with only partial observability and restricted inter-agent communication, an empirical Centralized Training with Decentralized Execution (CTDE) paradigm (Lowe et al., 2017) is employed to train well-coordinated decentralized policies by incorporating the global information while training in the simulation. While executing, agents make decisions based on the local observations according to the learned policies. CTDE allows agents to learn and construct individual

action-value functions, such that optimization at the individual level leads to optimization of the joint action-value function. This in turn, enables agents at execution time to select an optimal action simply by looking up the individual action-value functions, without having to refer to the joint one. Recent works including VDN and QMIX employ CTDE to train the scalable multiple agents with different ways of approximating the multiagent value function.

An important concept for such methods is decentralisability, also called Individual-Global-Max (IGM) (Son et al., 2019), which asserts that $\exists Q^i$, such that $\forall s, \vec{a}$:

$$\begin{aligned} \arg \max_{\vec{a}} Q^*(s, \vec{a}) = \\ (\arg \max_{a^1} Q^1(\tau^1, a^1) \dots \arg \max_{a^N} Q^N(\tau^N, a^N)), \end{aligned} \quad (1)$$

where τ^i is the history record of agent i 's observation o^i . While the containment is strict for partially observable setting, it can be shown that all tasks are decentralisable given full observability and sufficient representational capacity.

2.3. MARL Algorithms

2.3.1. VDN

Instead of letting each agent learn an individual action-value function Q^i independently as in IQL (Tan, 1993), VDN learns a centralized but factored Q_{tot} , where $Q_{tot}(s, \vec{a}) = \sum_i Q^i(s, a^i)$. By representing Q_{tot} as a sum of individual value functions Q^i that condition only on individual observations o^i and actions, a decentralised policy arises simply from each agent selecting actions greedily with respect to its Q^i . However, VDN assumes that the additivity exists when Q^i is evaluated based on o^i , which indeed makes an approximation and brings inaccuracy. VDN severely limits the complexity of centralized action-value functions and ignores any extra state information available during training.

2.3.2. QMIX

QMIX learns a monotonic multiagent Q-value approximation Q_{tot} (Rashid et al., 2018). QMIX factors the joint action-value Q_{tot} into a monotonic non-linear combination of individual Q-value Q^i of each agent which learns via a mixing network. The mixing network with non-negative weights produced by a hynernetwork is responsible for combing the agent's utilities for the chosen actions into $Q_{tot}(s, \vec{a})$. This nonnegativity ensures that $\frac{\partial Q_{tot}}{\partial Q^i} \geq 0$, which in turn guarantees the IGM property (Equation 1). The decomposition allows for an efficient, tractable maximization as it can be performed linearly from decentralized policies as well as the easy decentralize employment. During learning, the QMIX agents use ϵ -greedy exploration over their individual utilities to ensure sufficient exploration.

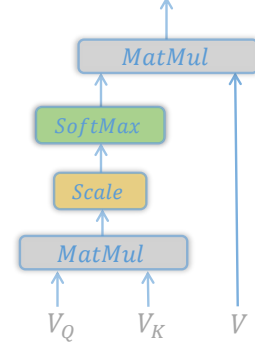


Figure 1. Attention Mechanism.

2.3.3. QTRAN

QTRAN further studies IGM. Theorem 1 in the QTRAN paper guarantees optimal decentralization by using linear constraints between agent utilities and joint action values, and avoid the representation limitations introduced by VDN and QMIX. However, the constraints on the optimization problem involved is computationally intractable to solve in discrete state-action spaces and is impossible given continuous state-action spaces. The authors propose two algorithms (QTRAN-base and QTRAN-alt) which relax these constraints using two L2 penalties but deviate QTRAN from the exact solution due to these relaxations. In practice, on the complex MARL domains (Samvelyan et al., 2019), QTRAN performs poorly (Mahajan et al., 2019).

2.4. Attention Mechanism

In recent years, attention mechanism (Vaswani et al., 2017) has been widely used in various research fields. The attention mechanism in deep learning originates from human visual attention and is trying to imitate the human's focusing process. The core goal behind both of them is to select the most relevant feature area which is more critical to the current task from the numerous information. Given the remarkable performance of attention mechanisms in various domains, more and more work relies on the idea of attention to deal with challenges of MAS. Figure 1 shows the particular attention proposed in (Vaswani et al., 2017). An attention function can be described as mapping a query and a set of key-value pairs to an output, where the query V_Q , keys V_K^j , values and output are all vectors. The output is computed as a weighted sum of the values, where each weight w_j assigned to each value is computed by a compatibility function of the query with the corresponding key.

$$w_j = \frac{\exp(f(V_Q, V_K^j))}{\sum_k \exp(f(V_Q, V_K^k))}, \quad (2)$$

where $f(V_Q, V_K^j)$ is the user-defined function to measure the importance of the corresponding value and the scaled dot-product is a common one. In practice, multi-head structure is usually employed to allow the model to focus on information from different representation sub-spaces.

3. Theory

In this section, we provide the theoretical foundation of our proposed Qatten model. We show that in the general framework of MARL without *any* additional assumption, when we investigate the global Q-value Q_{tot} **near maximum point in action space, the dependence of Q_{tot} on individual Q-value Q^i is approximately linear** (Theorem 2). The linear coefficients are proposed to be modeled in terms of attention mechanism to be elaborated in the Section 4, and the precision and effectiveness of this linear approximation is well validated in our experiment section (Section 5).

The functional relation between Q_{tot} and Q^i appears to be linear in action space, yet contains all the non-linear information. We show in Theorem 3 that the detailed structure of linear coefficients is related to all the non-linear dependence of Q_{tot} and Q^i . In other words, as functions of action variables, non-linear cross terms such as $Q^i Q^j$ turn out to be approximately linear.

We emphasize that our theory is based solely on conditions required in a general MARL setting. Our theory serves as an umbrella covering existing methods such as VDN, QMIX, QTRAN, including the (already) general framework IGM (Son et al., 2019), since all these methods require additional assumptions in MARL. In more precise terms, the Q-value $Q_{tot}(s, \vec{a})$ is a function on the state vector s and joint actions $\vec{a} = (a^1, \dots, a^N)$. We fix s and investigate the local behavior of Q_{tot} near a maximum point \vec{a}_o . Gradient vanishes in \vec{a}

$$\frac{\partial Q_{tot}}{\partial a^i}(s, \vec{a}_o) = 0 \quad (3)$$

so locally we have

$$Q_{tot}(s, \vec{a}) = Q_{tot}(s, \vec{a}_o) + \sum_{ij} \frac{\partial Q_{tot}}{\partial a^i \partial a^j}(a_o)(a^i - a_o^i)(a^j - a_o^j) + o(\|\vec{a} - \vec{a}_o\|^2). \quad (4)$$

One of the non-trivial points of our finding is that the second order term in Equation 4 has no cross terms.

Theorem 1. *The coefficients of $(a^i - a_o^i)(a^j - a_o^j)$ for $i \neq j$ in Equation 4 vanish, namely*

$$\frac{\partial Q_{tot}}{\partial a^i \partial a^j}(a_o) = 0.$$

When applied with the Implicit Function Theorem, Q_{tot} can

also be viewed as a function in terms of Q^i :

$$Q_{tot} = Q_{tot}(s, Q^1, Q^2, \dots, Q^n), \quad (5)$$

where $Q^i = Q^i(s, a^i)$. Our main result is that the major terms in Equation 4 ($Q_{tot}(\vec{a}_o)$ + second order term) coincide with a linear functional of Q^i , leaving the higher order terms $o(\|\vec{a} - \vec{a}_o\|^2)$ verified to be negligible in our experiments (Section 5).

Theorem 2. *There exist constants $c(s)$, $\lambda_i(s)$ (depending on state s), such that when we neglect higher order terms $o(\|\vec{a} - \vec{a}_o\|^2)$, the local expansion of Q_{tot} admits the following form*

$$Q_{tot}(s, \vec{a}) = c(s) + \sum_i \lambda_i(s) Q^i(s, a^i). \quad (6)$$

And in an cooperative setting, the constants $\lambda_i(s) \geq 0$.

The reason why in cooperative setting $\lambda_i(s)$ in Theorem 2 are non-negative is the the following. The common goal of agents is to maximize global Q-value Q_{tot} . If the coefficient $\lambda_i(s)$ of agent i is negative, increasing of Q^i will have a negative impact on the global value Q_{tot} . In this case, agent i sits in a competitive position against the whole group Q_{tot} . This is a violation of the cooperative assumption.

The major reason behind Theorem 2 is the following. Every agent i is connected to the whole group - an independent agent i should not be considered as a group member. This means mathematically that the variation of individual Q-value Q^i will have an impact (negative or positive) on the global Q-value Q_{tot} , that is

$$\frac{\partial Q_{tot}}{\partial Q^i} \neq 0$$

Now that gradient $\frac{\partial Q_{tot}}{\partial a^i}$ vanishes as in Eq. (3), it can be expanded by the chain rule as

$$\frac{\partial Q_{tot}}{\partial a^i} = \frac{\partial Q_{tot}}{\partial Q^i} \frac{\partial Q^i}{\partial a^i} = 0.$$

We conclude that

$$\frac{\partial Q^i}{\partial a^i} = 0, \quad (7)$$

namely each Q^i is locally quadratic in a^i . For a detailed proof of Theorem 2 see Appendix A.

In the next section, we propose to make use of the attention mechanism as universal function approximator (Yun et al., 2020) to approximate coefficients $\lambda_i(s)$ in the Theorem 2 (upto a normalization factor). The Universal Approximation Theorem for Transformer proved in (Yun et al., 2020) mathematically justifies our choice, where attention mechanism is shown to be responsible for Transformer's approximation

ability. The non-negativity of coefficients in cooperative setting coincide with the non-negativity of attention in Eq. (2).

Our second theoretical contribution is finer characterization of coefficients λ_i in Eq. (6).

Theorem 3. *We have the following finer structure of λ_i in Theorem 2*

$$\lambda_i(s) = \sum_h \lambda_{i,h}(s). \quad (8)$$

Namely, Eq. (6) becomes

$$Q_{tot}(s, \vec{a}) = c(s) + \sum_{i,h} \lambda_{i,h}(s) Q^i(s, a^i), \quad (9)$$

where $\lambda_{i,h}$ is a linear functional of all partial derivatives $\frac{\partial^h Q_{tot}}{\partial Q^{i_1} \dots \partial Q^{i_h}}$ of order h , and decays super-exponentially fast in h .

We remark when we employ attention mechanism to approximate λ_i , $\lambda_{i,h}$ is modelled as single-head attention. As far as we know, **this yields, for the first time, a theoretical explanation of multi-head construction in attention mechanism.** Since $\lambda_{i,h}$ decays fast in h , we stop the series at H (number of heads) for feasible computations in the next section. For a proof of Theorem 3 see Appendix A.

Our Eq. (9) appears to be linear in Q^i , yet contains all the non-linear information: the head coefficient $\lambda_{i,h}$ is a linear functional of all partial derivatives of order h , and corresponds to all cross terms $Q^{i_1} \dots Q^{i_h}$ of order h (e.g. $\lambda_{i,2}$ corresponds to second order non-linearity $Q^i Q^j$). This non-linearity includes, in particular, the special case of mixing network in QMIX model (Rashid et al., 2018). In fact, when expanding non-linear terms $Q^{i_1} \dots Q^{i_h}$, we find that its major part is identical to a linear term with coefficient $\lambda_{i,h}$, which contributes to a summand of the coefficient λ_i - this is how our proof of Theorem 3 works (Appendix A).

While our theory is developed locally, which usually requires an effective (convergence) radius of local approximations in action space, extensive experiments conducted in Section 5 show that this approximation radius readily covers a wide range of practical applications.

4. Framework

In this section, we propose the Q-value Attention network (Qatten), a practical deep Q-value decomposition network following the above theoretical formalization in Eq. (9). Figure 2 illustrates the overall architecture, which consists of agents' recurrent Q-value networks representing each agent's individual value function $Q^i(\tau^i, a^i)$ and the refined attention based value-mixing network to model the relation between Q_{tot} and individual Q-values. The attention-based mixing network takes individual agents' Q-values and local

information as input and mixes them with global state to produce the values of Q_{tot} .

We start from the fundamental theoretic formation of multiple linear mixing of Q_{tot} and Q^i . Letting the outer sum over h in Eq. (8), we have

$$Q_{tot} = c(s) + \sum_{h=1}^H \sum_{i=1}^N \lambda_{i,h}(s) Q^i. \quad (10)$$

For each h , the inner linear sum operation can be implemented using the differentiable key-value memory model (Graves et al., 2014; Oh et al., 2016) to establish the linear relations from the individuals to the global. Specifically, we pass the similarity value between the global state's embedding vector $e_s(s)$ and the individual properties' embedding vector $e_i(o^i)$ into a softmax.

$$\lambda_{i,h} \propto \exp(e_s^T W_{k,h}^T W_{q,h} e_s), \quad (11)$$

where $W_{q,h}$ transforms e_s into the global query and $W_{k,h}$ transforms e_i into the key of each agent. The e_s and e_i could be obtained by a one or two-layer embedding transformation for s and each o^i . To increase the **non-linearity** of Q_{tot} and Q^i , we could assign each agent's Q-value Q^i to its o^i when performing self-attention. As o^i is replaced by (o^i, Q^i) and the self-attention function uses the softmax activation, Qatten could represent the non-linear combination of Q_{tot} and Q^i . Next, for the outer sum over h , we use multiple attention heads to implement the approximations of different orders of partial derivatives. By summing up the head Q-values Q^h from the different heads, we get

$$Q_{tot} = c(s) + \sum_{h=1}^H Q^h, \text{ where } Q^h = \sum_{i=1}^N \lambda_{i,h} Q^i. \quad (12)$$

H is the number of attention heads. Lastly, the first term $c(s)$ in Eq. (9) could be learned by a neural network with the global state s as input.

As implied by our theory, Qatten naturally holds the monotonicity and achieves IGM property between Q_{tot} and Q^i .

$$\frac{\partial Q_{tot}}{\partial Q^i} \geq 0, \forall i \in \{1, 2, \dots, N\}, \quad (13)$$

Thus, Qatten allows tractable maximisation of the joint action-value in off-policy learning, and guarantees consistency between the centralized and decentralized policies.

Weighted Head Q-value In previous descriptions, we directly add the Q-value contribution from different heads. But if the environment becomes complex, we could assign weights w_h for the Q-values from different heads to capture more complicated relations. To ensure monotonicity, we

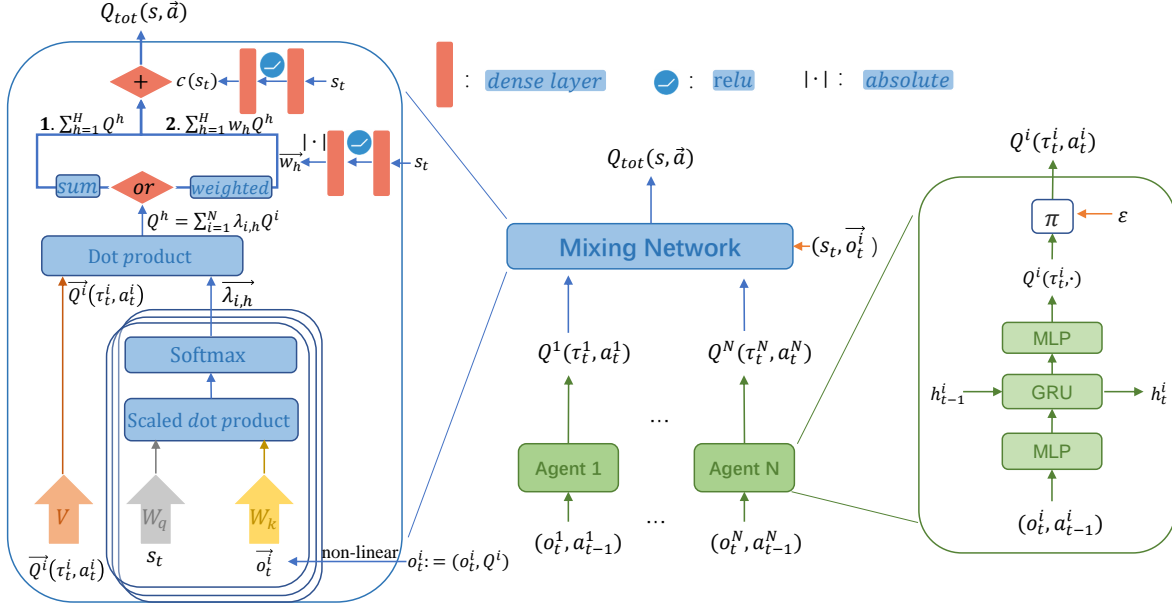


Figure 2. The overall architecture of Qatten. The right is agent i 's recurrent deep Q-network, which receives last hidden states h_{t-1}^i and current local observations o_t^i as inputs. Last action a_{t-1}^i is also inputted to enhance the local observation. The left is the mixing network of Qatten, which mixes $Q^i(\tau_t^i, a_t^i)$ together with s_t . At time t , s_t could be represented by the joint unit features or joint observations.

retrieve these head Q-value weights with an absolute activation function from a two-layer feed-work network f^{NN} , which adjusts head Q-values based on global states s .

$$Q_{tot} = c(s) + \sum_{h=1}^H w_h \sum_{i=1}^N \lambda_{i,h} Q^i, \quad (14)$$

where $w_h = |f^{NN}(s)|_h$. Compared with directly summing up head Q-values, the weighted head Q-values relaxes the upper bound and lower bound of Q_{tot} imposed by attention.

5. Experimental Evaluation

5.1. Settings

In this section, we evaluate Qatten in the StarCraft II decentralized micromanagement tasks and use StarCraft Multi-Agent Challenge (SMAC) environment (Samvelyan et al., 2019) as our testbed, which has become a common-used benchmark for evaluating state-of-the-art MARL approaches such as COMA (Foerster et al., 2018), QMIX (Rashid et al., 2018) and QTRAN (Son et al., 2019). We train multiple agents to control allied units respectively, while the enemy units are controlled by a built-in hand-crafted AI. At the beginning of each episode, the enemy units are going to attack the allies. Proper micromanagement of units during battles are needed to maximize the damage to enemy units while minimizing damage received, hence requires a range of coordination skills such as focusing fire and avoiding overkill. Learning these diverse

cooperative behaviors under partial observation is challenging. All the results are averaged over 5 runs with different seeds. Training and evaluation schedules such as the testing episode number and training hyper-parameters are kept the same as QMIX in SMAC. For the attention part, the embedding dim for the query (s) and key o^i is 32, and the head number is set to 4. More details are provided in Appendix.

Table 1. Maps in hard and super hard scenarios.

Name	Ally Units	Enemy Units	Type
5m_vs.6m (hard)	5 Marines	6 Marines	Asymmetric Homogeneous
3s_vs.5z (hard)	3 Stalkers	5 Zealots	Asymmetric Heterogeneous
2c_vs.64zg (hard)	2 Colossi	64 Zerglings	Asymmetric Heterogeneous
bane_vs.bane (hard)	4 Banelings	4 Banelings	Symmetric Heterogeneous
3s5z_vs.3s6z (super hard)	3 Stalkers	3 Stalkers	Asymmetric Heterogeneous
	5 Zealots	6 Zealots	
MMM2 (super hard)	1 Medivac	1 Medivac	Asymmetric Heterogeneous
	2 Marauders	3 Marauders	
	7 Marines	8 Marines	

According to the map characters and learning performance of algorithms, SMAC divides these maps into three levels: easy scenarios, hard scenarios and super hard scenarios. All map scenarios are of different agent number or agent type. The easy scenarios include 2s_vs.1sc, 2s3z, 3s5z, 1c3s5z and 10m_vs.11m. Here we briefly introduce the hard scenarios and super hard scenarios in Table 1.

In the hard scenarios, 5m_vs.6m requires the precise control such as focusing fire and consistent walking to win. In 3s_vs.5z, since Zealots counter Stalkers, the only winning strategy is to kite the enemy around the map and kill them one after another. In 2c_vs.64zg, 64 enemy units make the action space of the agents the largest among all scenarios. In bane_vs.bane, the strategy of winning is to correctly use the Banelings to destroy as many enemies as possible. For super hard scenarios, the key winning strategy of MMM2 is that the Medivac heads to enemies first to absorbing fire and then retreats to heal the right ally with the least health. As the most difficult scenarios, 3s5z_vs.3s6z may require a better exploration mechanism while training.

5.2. Validation

5.2.1. EASY SCENARIOS

First, we test Qatten on the easy scenarios to validate its effectiveness. Table 2 shows the median test win rate of different MARL algorithms. These results demonstrate that Qatten achieves competitive performance with QMIX and other popular methods. Qatten could master these easy tasks and also works well in heterogeneous and asymmetric settings. COMA’s poor performance results from the sample inefficient on-policy learning and the naive critic structure. Except 2s_vs.1sc and 2s3z, IDL’s win percentage is quite low as directly using global rewards to update policies brings the non-stationary, which becomes severe when the number of agents increases. QTRAN also performs not well, as the practical relaxations impede the exactness of its updating.

Table 2. Median performance of the test win percentage.

Scenario	Qatten	QMIX	COMA	VDN	IDL	QTRAN
2s_vs.1sc	100	100	97	100	100	100
2s3z	97	97	34	97	75	83
3s5z	94	94	0	84	9	13
1c3s5z	97	94	23	84	11	67
10m_vs.11m	97	94	5	94	19	59

5.2.2. HARD SCENARIOS

Next, we test Qatten on the hard scenarios. Results are presented in Figure 3 as 25%-75% percentile is shaded. To summarize, these scenarios reflects different challenges, and existing approaches fails to achieve consistent performance as they do in the easy scenarios. For example, in bane_vs.bane, it is surprising that IQL performs quite well (rank 2th) as there are 24 agents while QMIX cannot learn steadily. The reason is that the global Q-value heavily depends on the 4 Banelings among 24 agents as they are vital to win the battle, thus IQL only needs to learn the well coordinated policies for 4 Banelings while QMIX cannot easily find the appropriate formation for Q_{tot} and Q_i . In the four

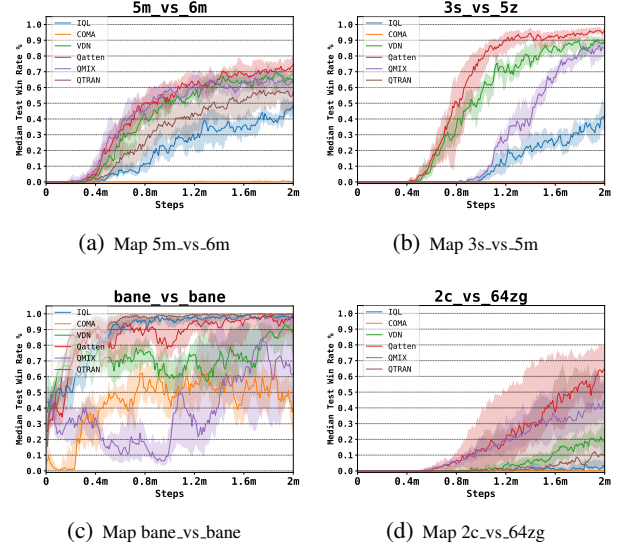


Figure 3. Median win percentage on the hard scenarios.

maps, VDN and QMIX show advantages over each other on different maps. In contrast, Qatten consistently beats all other approaches in these hard maps, which validates the effectiveness of its general mixing formula of Q_{tot} and Q_i .

5.2.3. SUPER HARD SCENARIOS

Finally, we test Qatten on the super hard scenarios as shown in Figure 4 where 25%-75% percentile is shaded. Due to the difficulty and complexity, we augment Qatten with weighted head Q-values. In MMM2, Qatten masters the winning strategy by heading Medivac to absorb damage and then retreating it and exceeds QMIX by a large margin. The 3s5z_vs.3s6z is another more challenging scenario and all existing approaches fails. In contrast, our approach Qatten can win approximately 16% after 2 million steps of training.

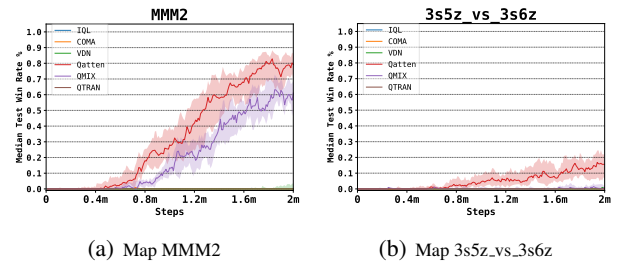


Figure 4. Median win percentage on the super hard scenarios.

5.3. Ablation Study

We investigate the influence of weighted head Q-values using three difficult scenarios (2c_vs.64zg, MMM2 and 3s5z_vs.3s6z) as demonstrated in previous experiments for

illustration. For clarity, the basic Qatten without weighted head Q-value is called Qatten-base while Qatten with weighted head Q-value is called Qatten-weighted. Figure 5 shows the ablation results and 25%-75% percentile is shaded. As we can see, the weighted head Q-values can leverage the performance of Qatten-base on these difficult scenarios. It shows that this mechanism may capture sophisticated relations between Q_{tot} and Q^i more accurately with w_h adjusting head weights flexibly. Specifically, in MMM2, Qatten is also augmented with the non-linearity trick which adds Q^i into o^i while performing self-attention.

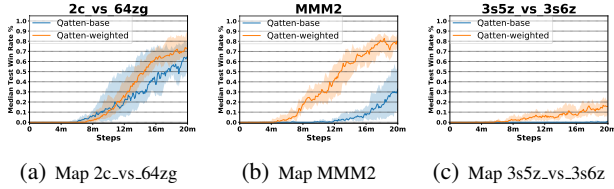


Figure 5. Ablation study of Qatten on three difficult scenarios.

5.4. Attention Analysis

Next, we visualize the attention weights ($\lambda_{i,h}$) on each step during a battle to better understand Qatten’s learning process. We choose two representative maps 5m_vs_6m and 3s5z_vs_3s6z for illustration and the attention weight heat map of each head for each map is shown in Figure 6(a-b) and Figure 6(c-d) respectively. For 5m_vs_6m, the most important trick to win is to avoid being killed and focusing fire to kill enemy. From Figure 6(a), we see allies have similar attention weights, which means that Qatten indicates an almost equally divided Q_{tot} for agents. This is because that each ally marine plays similar roles on this homogeneous scenario. This may also explain the fact that VDN could slightly outperform QMIX when the weights of each Q^i is roughly equal. But we still find some tendencies of Qatten. One main tendency is that, the only alive unit (agent 0) receives the highest weight in the later steps of the episode, which encourages agents to survive for winning. Thus, with the refined attention mechanism adjusting weights with minor difference, Qatten performs best.

Then we analyse another map 3s5z_vs_3s6z and the attention heat map is shown in Figure 6(c). After analyzing the correlation of attention weights and agent features, we notice that Head 1 focuses on the output damage. Units with high CoolDown (indicating just fired) receives high attention values. Head 1 and 2 tend to focus on the Stalker agents (Agent 0, 1 and 2) while Stalkers (Agent 3-7) almost receives no attention at the beginning. While Stalker agent 1 with high health receives attention from head 1 and 2, Zealot agent 6 with high health receives attention from head 0 and 3. In summary, attention weights on map 3s5z_vs_3s6z

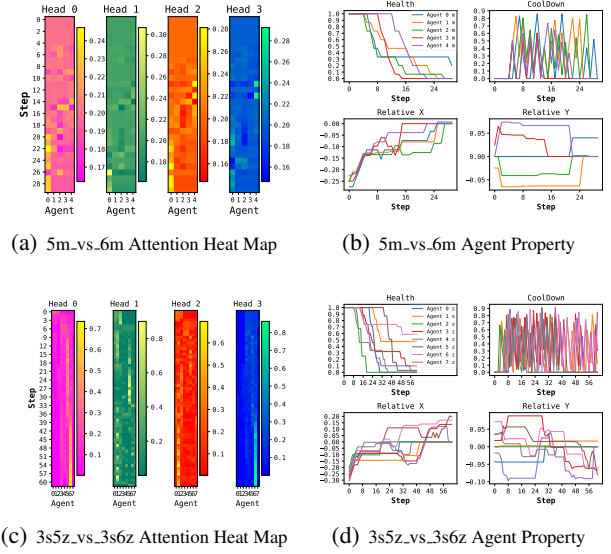


Figure 6. Attention weights on 5m_vs_6m and 3s5z_vs_3s6z. Steps increase from top to the bottom in the attention heat maps. Horizontal ordination indicates the agent id under each head.

are changing violently. As the battle involves highly fluctuant dynamics, VDN which statically decomposes Q_{tot} equally thus cannot adapt to the complex scenarios. Similarly, QMIX with a rough and implicit approximation way also fails. In contrast, Qatten could approximate the sophisticated relations between Q^i and Q_{tot} with different attention heads to capture different features in sub-spaces.

6. Conclusion and Future Work

In this paper, we propose the novel Q-value Attention network for the multiagent Q-value decomposition problem. For the first time, we derive a theoretic linear decomposition formula of Q_{tot} and Q^i which covers previous methods and provide a theoretical explanation of multi-head structure. To approximate each term of the decomposition formula, we introduce multi-head attention to establish the mixing network. Furthermore, Qatten could be enhanced by weighted head Q-values. Experiments on the standard MARL benchmark show that our method obtains the best performance on almost all maps and the attention analysis gives the intuitive explanations about the weights of each agent while approximating Q_{tot} and, to some degree, reveals the internal workflow of the Q_{tot} ’s approximation from Q^i .

For future work, improving Qatten by combining with explicit exploration mechanism on difficult MARL tasks is a straightforward direction. Besides, incorporating recent progresses of attention to adapt Qatten into large-scale settings where hundreds of agents exist is also promising.

References

- Busoniu, L., Babuska, R., and De Schutter, B. A comprehensive survey of multiagent reinforcement learning. *IEEE Transactions on Systems, Man, and Cybernetics*, 38(2): 156–172, 2008.
- Cao, Y., Yu, W., Ren, W., and Chen, G. An overview of recent progress in the study of distributed multi-agent coordination. *IEEE Transactions on Industrial Informatics*, 9(1):427–438, 2012.
- Foerster, J. N., Farquhar, G., Afouras, T., Nardelli, N., and Whiteson, S. Counterfactual Multi-Agent Policy Gradients. In *Proceedings of the 32nd AAAI Conference on Artificial Intelligence*, 2018.
- Graves, A., Wayne, G., and Danihelka, I. Neural Turing Machines. *arXiv:1410.5401 [cs]*, December 2014. URL <http://arxiv.org/abs/1410.5401>. arXiv: 1410.5401.
- Gupta, J. K., Egorov, M., and Kochenderfer, M. Cooperative multi-agent control using deep reinforcement learning. In *Proceedings of the 16th International Conference on Autonomous Agents and MultiAgent Systems*, pp. 66–83, 2017.
- Littman, M. L. Markov games as a framework for multi-agent reinforcement learning. In *Machine Learning Proceedings*, pp. 157–163. Elsevier, 1994. doi: 10.1016/B978-1-55860-335-6.50027-1.
- Lowe, R., WU, Y., Tamar, A., Harb, J., Pieter Abbeel, O., and Mordatch, I. Multi-Agent Actor-Critic for Mixed Cooperative-Competitive Environments. In *Proceedings of the 31st Advances in Neural Information Processing Systems*, pp. 6379–6390. Curran Associates, Inc., 2017.
- Mahajan, A., Rashid, T., Samvelyan, M., and Whiteson, S. MAVEN: Multi-Agent Variational Exploration. In Wallach, H., Larochelle, H., Beygelzimer, A., Alch-Buc, F. d., Fox, E., and Garnett, R. (eds.), *Proceedings of the 32nd International Conference on Neural Information Processing Systems*, pp. 7611–7622. Curran Associates, Inc., 2019.
- Matignon, L., Laurent, G. J., and Le Fort-Piat, N. Independent reinforcement learners in cooperative Markov games: a survey regarding coordination problems. *The Knowledge Engineering Review*, 27(1):1–31, 2012.
- Oh, J., Chockalingam, V., Singh, S., and Lee, H. Control of memory, active perception, and action in minecraft. In *Proceedings of the 33rd International Conference on International Conference on Machine Learning*, ICML’16, pp. 2790–2799. JMLR.org, 2016. URL <http://dl.acm.org/citation.cfm?id=3045390.3045684>.
- Palmer, G., Tuyls, K., Bloembergen, D., and Savani, R. Lenient multi-agent deep reinforcement learning. In *Proceedings of the 17th International Conference on Autonomous Agents and MultiAgent Systems*, pp. 443–451, 2018.
- Rashid, T., Samvelyan, M., Witt, C. S. d., Farquhar, G., Foerster, J. N., and Whiteson, S. QMIX: Monotonic Value Function Factorisation for Deep Multi-Agent Reinforcement Learning. In *Proceedings of the 35th International Conference on Machine Learning*, pp. 4292–4301, 2018.
- Samvelyan, M., Rashid, T., de Witt, C. S., Farquhar, G., Nardelli, N., Rudner, T. G. J., Hung, C.-M., Torr, P. H. S., Foerster, J., and Whiteson, S. The StarCraft Multi-Agent Challenge. In *arXiv:1902.04043 [cs, stat]*, February 2019. URL <http://arxiv.org/abs/1902.04043>. arXiv: 1902.04043.
- Schroeder de Witt, C., Foerster, J., Farquhar, G., Torr, P., Boehmer, W., and Whiteson, S. Multi-Agent Common Knowledge Reinforcement Learning. In Wallach, H., Larochelle, H., Beygelzimer, A., Alch-Buc, F. d., Fox, E., and Garnett, R. (eds.), *Proceedings of the Advances in Neural Information Processing Systems 32*, pp. 9924–9935. Curran Associates, Inc., 2019.
- Son, K., Kim, D., Kang, W. J., Hostallero, D. E., and Yi, Y. QTRAN: Learning to Factorize with Transformation for Cooperative Multi-Agent Reinforcement Learning. In Chaudhuri, K. and Salakhutdinov, R. (eds.), *Proceedings of the 36th International Conference on Machine Learning*, volume 97 of *Proceedings of Machine Learning Research*, pp. 5887–5896, Long Beach, California, USA, June 2019. PMLR.
- Sunehag, P., Lever, G., Gruslys, A., Czarnecki, W. M., Zambaldi, V., Jaderberg, M., Lanctot, M., Sonnerat, N., Leibo, J. Z., Tuyls, K., and Graepel, T. Value-Decomposition Networks For Cooperative Multi-Agent Learning Based On Team Reward. In *Proceedings of the 17th International Conference on Autonomous Agents and MultiAgent Systems*, AAMAS ’18, pp. 2085–2087, Richland, SC, 2018. International Foundation for Autonomous Agents and Multiagent Systems. URL <http://dl.acm.org/citation.cfm?id=3237383.3238080>.
- Tan, M. Multi-agent reinforcement learning: Independent vs. cooperative agents. In *Proceedings of the 10th International Conference on Machine Learning*, pp. 330–337. Morgan Kaufmann, 1993.
- Vaswani, A., Shazeer, N., Parmar, N., Uszkoreit, J., Jones, L., Gomez, A. N., Kaiser, L., and Polosukhin, I. Attention is All you Need. In Guyon, I., Luxburg, U. V., Bengio, S., Wallach, H., Fergus, R., Vishwanathan, S.,

and Garnett, R. (eds.), *Proceedings of the 30th International Conference on Neural Information Processing Systems*, pp. 5998–6008. Curran Associates, Inc., 2017. URL <http://papers.nips.cc/paper/7181-attention-is-all-you-need.pdf>.

Ying, W. and Sang, D. Multi-agent framework for third party logistics in e-commerce. *Expert Systems with Applications*, 29(2):431–436, 2005.

Yun, C., Bhojanapalli, S., Rawat, A. S., Reddi, S. J., and Kumar, S. Are transformers universal approximators of sequence-to-sequence functions? In *Proceedings of the 8th International Conference on Learning Representations*, 2020.

A. Proofs

Proof of Theorem 1:

Proof. This follows directly from Theorem 2: Q^i is only related to a^i , therefore, when a^i is expanded from Q^i , there is no terms $a^i a^j$ for $i \neq j$. \square

Proof of Theorem 2:

Proof. Theorem 2 follows directly from Theorem 3, and its proof is identical to that of Theorem 3 as well. Please see the proof of Theorem 3 for completeness. \square

Proof of Theorem 3:

Proof. We expand Q_{tot} in terms of Q^i

$$\begin{aligned} Q_{tot} = & \text{constant} + \sum_i \mu_i Q^i + \sum_{ij} \mu_{ij} Q^i Q^j + \dots \\ & + \sum_{i_1 \dots i_k} \mu_{i_1 \dots i_k} Q^{i_1} \dots Q^{i_k} + \dots \end{aligned} \quad (15)$$

where

$$\mu_i = \frac{\partial Q_{tot}}{\partial Q^i}, \mu_{ij} = \frac{1}{2} \frac{\partial^2 Q_{tot}}{\partial Q^i \partial Q^j},$$

and in general

$$\mu_{i_1 \dots i_k} = \frac{1}{k!} \frac{\partial^k Q_{tot}}{\partial Q^{i_1} \dots \partial Q^{i_k}}.$$

We will simply take

$$\lambda_{i,1} = \mu_i$$

in Theorem 3.

Recall that every agent i is related to the whole group, and thus its interest must be associated to that of the group. That is to say, variations of each Q^i will have an impact on Q_{tot} :

$$\frac{\partial Q_{tot}}{\partial Q^i} \neq 0.$$

Now that gradient $\frac{\partial Q_{tot}}{\partial a^i}$ vanishes as in Eq. (3), it can be expanded by the chain rule as

$$\frac{\partial Q_{tot}}{\partial a^i} = \frac{\partial Q_{tot}}{\partial Q^i} \frac{\partial Q^i}{\partial a^i} = 0.$$

We conclude that

$$\frac{\partial Q^i}{\partial a^i}(a_o) = 0.$$

This is exactly Equation 7, which we copy here for the reader's convenience. Consequently, we have local expansion

$$Q^i(a^i) = \alpha_i + \beta_i(a^i - a_o^i)^2 + o((a^i - a_o^i)^2).$$

Now we apply the equation above to the second order term in Equation 15:

$$\begin{aligned} & \sum_{ij} \mu_{ij} Q^i Q^j \\ = & \sum_{ij} \mu_{ij} (\alpha_i + \beta_i(a^i - a_o^i)^2)(\alpha_j + \beta_j(a^j - a_o^j)^2) + o(\|a - a_o\|^2) \\ = & \sum_{ij} \mu_{ij} \alpha_i \alpha_j + 2 \sum_{ij} \mu_{ij} \alpha_j \beta_i (a^i - a_o^i)^2 + o(\|a - a_o\|^2) \\ = & \sum_{ij} \mu_{ij} \alpha_i \alpha_j + 2 \sum_{ij} \mu_{ij} \alpha_j (Q^i - \alpha_i) + o(\|a - a_o\|^2) \\ = & - \sum_{ij} \mu_{ij} \alpha_i \alpha_j + 2 \sum_{ij} \mu_{ij} \alpha_j Q^i + o(\|a - a_o\|^2) \end{aligned}$$

Therefore, we will take

$$\lambda_{i,2} = 2 \sum_j \mu_{ij} \alpha_j.$$

In general, we have

$$\mu_{i_1 \dots i_k} = \frac{1}{k!} \frac{\partial^k Q_{tot}}{\partial Q^{i_1} \dots \partial Q^{i_k}}$$

and

$$\begin{aligned} \sum_{i_1, \dots, i_k} \mu_{i_1 \dots i_k} Q^{i_1} \dots Q^{i_k} &= -(k-1) \sum_{i_1, \dots, i_k} \mu_{i_1 \dots i_k} \\ &+ k \sum_{i_1, \dots, i_k} \mu_{i_1 \dots i_k} \alpha_{i_1} \dots \alpha_{i_{k-1}} Q^{i_k} + o(\|a - a_o\|^2) \end{aligned}$$

so we take

$$\lambda_{i,k} = k \sum_{i_1, \dots, i_k} \mu_{i_1 \dots i_{k-1} i} \alpha_{i_1} \dots \alpha_{i_{k-1}}.$$

The convergence of the series $\sum_k \lambda_{i,k}$ only requires mild conditions, e.g. boundedness or even small growth of partial derivatives $\frac{\partial^k Q_{tot}}{\partial Q^{i_1} \dots \partial Q^{i_k}}$ in terms of k .

Both Theorem 2 and Theorem 3 follow from this proof. \square

B. Experimental Settings

We follow the settings of SMAC (Samvelyan et al., 2019), which could be referred in the SMAC paper. For clarity and completeness, we state these environment details again.

B.1. States and Observations

At each time step, agents receive local observations within their field of view. This encompasses information about the map within a circular area around each unit with a radius equal to the sight range, which is set to 9. The sight range makes the environment partially observable for agents. An agent can only observe others if they are both alive and located within its sight range. Hence, there is no way for agents to distinguish whether their teammates are far away or dead. If one unit (both for allies and enemies) is dead or unseen from another agent’s observation, then its unit feature vector is reset to all zeros. The feature vector observed by each agent contains the following attributes for both allied and enemy units within the sight range: distance, relative x, relative y, health, shield, and unit type. If agents are homogeneous, the unit type feature will be omitted. All Protos units have shields, which serve as a source of protection to offset damage and can regenerate if no new damage is received. Lastly, agents can observe the terrain features surrounding them, in particular, the values of eight points at a fixed radius indicating height and walkability.

The global state is composed of the joint unit features of both ally and enemy soldiers. Specifically, the state vector includes the coordinates of all agents relative to the centre of the map, together with unit features present in the observations. Additionally, the state stores the energy/cooldown of the allied units based the unit property, which represents the minimum delay between attacks/healing. All features, both in the global state and in individual observations of agents, are normalized by their maximum values.

B.2. Action Space

The discrete set of actions which agents are allowed to take consists of move[direction], attack[enemy id], stop and no-op. Dead agents can only take no-op action while live agents cannot. Agents can only move with a fixed movement amount 2 in four directions: north, south, east, or west. To ensure decentralization of the task, agents are restricted to use the attack[enemy id] action only towards enemies in their shooting range. This additionally constrains the ability of the units to use the built-in attack-move macro-actions on the enemies that are far away. The shooting range is set to be 6 for all agents. Having a larger sight range than a shooting range allows agents to make use of the move commands before starting to fire. The unit behavior of automatically responding to enemy fire without being explicitly ordered is also disabled. As healer units, Medivacs use heal[agent.id] actions instead of attack[enemy_id].

B.3. Rewards

At each time step, the agents receive a joint reward equal to the total damage dealt on the enemy units. In addition, agents receive a bonus of 10 points after killing each opponent, and 200 points after killing all opponents for winning the battle. The rewards are scaled so that the maximum cumulative reward achievable in each scenario is around 20.

B.4. Training Configurations

The training time is about 8 hours to 18 hours on these maps (GPU Nvidia RTX 2080 and CPU AMD Ryzen Threadripper 2920X), which is ranging based on the agent numbers and map features of each map. The number of the total training steps is about 2 million and every 10 thousand steps we train and test the model. When training, a batch of 32 episodes are retrieved from the replay buffer which contains the most recent 5000 episodes. We use ϵ -greedy policy for exploration. The starting exploration rate is set to 1 and the end exploration rate is 0.05. Exploration rate decays linearly at the first 50 thousand steps. We keep the default configurations of environment parameters.

Table 3. The network configurations of Qatten’s mixing network.

Qatten mixing network configurations	Value
Query embedding layer number	2
Unit number in query embedding layer 1	64
Activation after query embedding layer 1	Relu
Unit number in query embedding layer 2	32
Key embedding layer number	1
Unit number in key embedding layer 1	32
Head weight layer number	2
Unit number in head weight layer 1	64
Activation after head weight layer 1	Relu
Unit number in head weight layer 2	4
Attention head number	4
Constant value layer number	2
Unit number in constant value layer 1	32
Activation after constant value layer 1	Relu
Unit number in constant value layer 2	1

B.5. Mixing Network Hyper-parameters

We adopt the Python MARL framework (PyMARL) (Samvelyan et al., 2019) on the github to develop our algorithm. The hyper-parameters of training and testing configu-

rations are the same as in SMAC (Samvelyan et al., 2019) and could be referred in the source codes. Here we list the special parameters of Qatten’s mixing network in Table 3.

B.6. Win Percentage Table of All Maps

We here give the median win rates of all methods on the scenarios presented in our paper. In MMM2 and 3s5z_vs_3s6z, we augment Qatten with the weighted head Q-values. Other maps are reported by the win rates based on the original Qatten (Qatten-base). We could see Qatten obtains the best performance on almost all the map scenarios.

Table 4. Median performance of the test win percentage.

Scenario	Qatten	QMIX	COMA	VDN	IDL	QTRAN
2s_vs_1sc	100	100	97	100	100	100
2s3z	97	97	34	97	75	83
3s5z	94	94	0	84	9	13
1c3s5z	97	94	23	84	11	67
5m_vs_6m	74	63	0	63	49	57
3s_vs_5z	96	85	0	87	43	0
bane_vs_bane	97	62	40	90	97	100
2c_vs_64zg	65	45	0	19	2	10
MMM2	79	61	0	0	0	0
3s5z_vs_3s6z	16	1	0	0	0	0